Long Term Corrosion Protection of Epoxy Coating Containing Tetraaniline Nanofiber

Feng Yang[1], Tong Liu[1,2], Jingyu Li[1,2], Haichao Zhao[2,]*

[1] Shenyang University of Chemistry and Technology, Shenyang, 110142, P. R. China
[2] Key Laboratory of Marine Materials and Related Technologies, Zhejiang Key Laboratory of Marine Materials and Protective Technologies, Ningbo Institute of Materials Technology and Engineering, Chinese Academy of Sciences, Ningbo 315201, P. R. China.
[*]E-mail: zhaohaichao@nimte.ac.cn

A supermolecular assembly chemistry was applied to aniline based oligomer, tetraaniline (TANI), in 1 M HCl aqueous solution to obtain nanofibrous emeraldine salt of TANI (TANI-ES), making it suitable as novel anticorrosive inhibitor for primer coatings. Epoxy coating pigmented with 0.5 wt% and 1 wt% TANI-ES were then prepared by curing reaction of epoxy E44, polyamide hardener with the existence of TANI-ES. The corrosion behavior of the coatings without and with 0.5 wt% and 1.0 wt% TANI-ES on Q235 steel in the 3.5 wt% NaCl solution was investigated by open circuit potential (OCP) test, electrochemical impedance spectroscopy (EIS) measurements, scanning vibrating electrode technique (SVET) as well as salt spray test. Results suggested that synthesized epoxy composite coatings, particularly with 0.5 wt% TANI-ES nanofiber coating, exhibited exceptional anticorrosion capability compared with the pure epoxy E44 coating. The salt spray test exhibited that 0.5 wt% conducting polymer coating possessed excellent salt-fog-resistance property with slight rust formation and blistering resistance on the steel sheets.

1. INTRODUCTION

Epoxy resin have been developed over years as a primer coating to extend the service life of metal by improving its corrosion durability. To provide reliable and long-term corrosion protection, metal and metal oxide based particles, in most case, have been considered to incorporate into the epoxy matrix due to their beneficial electrical and mechanical properties [1-4]. However, most developed pigments are toxic, contributing to detrimental effects on both the environment and human health. Along with the more strict environment regulations, it is encouraging to develop more

environmentally compatible anticorrosive pigments that can replace current toxic pigments in coating formulations [5-7].

Over the last several decades, intrinsically conducting polymers (ICPs) have been validated as one of the most efficient polymeric corrosive inhibitors for corrosion protection of metallic substrate in aggressive environment [8-10]. ICPs can be directly formed by electropolymerization of its monomeric units on the surface of metal in the electrolyte [11-13]. Nevertheless, the most applicable and successful ICPs is used as additive for epoxy resin to form a composite coating, which protect metal again corrosion in a synergistic manner by combination of the barrier effects of epoxy film and corrosion inhibitive properties of ICPs [10, 14]. At present, polyaniline is the ICP most investigated for the anticorrosive applications owing to its simplicity of synthesis, chemical stability and relative high conductivity. Polyaniline can passivate the steel substrate to form a $Fe_3O_4/\gamma\text{-}Fe_2O_3$ barrier film, preventing a high diffusion resistance against corrosive species [15, 16]. Because unsubstituted PANI is immiscible with epoxy resin and the aggregated PANI particles may introduce localized defects, the uniform dispersion of PANI in the epoxy coating matrix is directly relevant to the corrosion protect performance [17, 18]. In this respect, the addition of processable nanoparticulate or nanofiberous PANI into the epoxy matrix offers advantages to enhancing the integrity and durability of coatings. We and other groups have demonstrated that the nanosized PANI can not only act as corrosion inhibitor, but also as a nanoreinforcing filler by decreasing the microcavities and zigzagging the diffusion path for deleterious species [17-22].

Recently, supramolecular assembly has emerged as a promising technology for creating nanostructured materials of π-conjugated molecules through a series of nonconvalent interactions such as hydrogen bonding, ionic interaction, π-π stacking and electrostatic interaction [23, 24]. Among the family of π-conjugated molecules, aniline based oligomer, tetraaniline (TANI), has been assembled into 1-D nanowires, 2-D nanoribbons, 3-D rectangular nanoplates and nanoflowers through solvent exchange process assisted by doping acid such as HCl, HNO_3, $HClO_4$ and H_2SO_4 [25-28]. The aim of this research is to prepare processable tetraniline nanofiber and apply it as a pigment for the epoxy coating. The effect of TANI nanofiber on corrosion resistance of resulting epoxy coating was evaluated by conventional electrochemical measurements including open circuit potential, electrochemical impedance spectroscopy (EIS), and scanning vibrating electrode technique (SVET) as well as salt spray test.

2. EXPERIMENTAL SECTION

2.1 Materials

Epoxy resin (E44) and amine curing agent were provided from Yunda Chemical Co. Ltd. China. 4-aminodiphenylamine, ammonium persulfate (APS) and ammonia solution were purchased by Aladdin Industrial Corporation. Acetone, absolute ethanol and hydrochloric acid were provided by Sinopharm Chemical Reagent Co. Ltd. Chemicals and reagents were used by no purification. The Q235 steel electrodes were used as the substrate in this work.

2.2 Preparation of TANI-EB

The Tetraaniline Emeraldine Base (TANI-EB) was synthesized by following published literature procedures [29, 30]. Firstly, 4-aminodiphenylamine (60 mmol, 11.0544 g) was completely dissolved in the acetone (300 mL), 1 mol/L HCl (75 mL) and deionized water (300 mL) in an ice-bath. Then, 1 mol/L HCl (150 mL) with ammonium persulfate (APS) (40 mmol) was added dropwise into the as-prepared solution with vigorous stirring for 1 hour and continued to stir for 3 hours. The semi-product was collected by Buchner funnel and dedoped by dissolved in 50 mL NH_4OH and 300 mL deionized water with stirring for 6h. The TANI-EB sample was obtained via filtration and thorough washing by deionized water. Finally, the as-synthetic TANI-EB was dried in the vacuum oven at 50 °C for 72 h.

2.3 Preparation of self-assembly TANI-ES nanofiber

Tetraaniline Emeraldine Salt (TANI-ES) nanofibers were prepared by a rapid self-assembled polymerization method. Preparation schematic representation of TANI-ES nanofiber was showed in Fig. 1. In brief, 2.0 mg of finely powdered Tetraaniline Emeraldine Base (TANI-EB) was added to solvent mixture composed of ethanol (2.0 mL) and 1 mol/L HCl (8.0 mL). The mixed liquor was under ultrasonic irradiation for 2 mins and green floccus emerged rapidly via speedy protonation. Then TANI-ES nanofibers sizing agent was obtained by centrifugation and the product can be readily separated by centrifugal process. Finally, the product was dried to a constant weight as powder in vacuum at 40 °C. As shown in Fig. 1, the as-prepared TANI-EB and TANI-ES nanofiber, in ethanol of a concentration of 0.1 mg/mL, exhibited wathet blue and dark green. Generally, this sharp color change (from blue to green) implied nanofibers were doped successfully (measured conductivity value of as-prepared TANI nanofibers: 90.78 mS/cm).
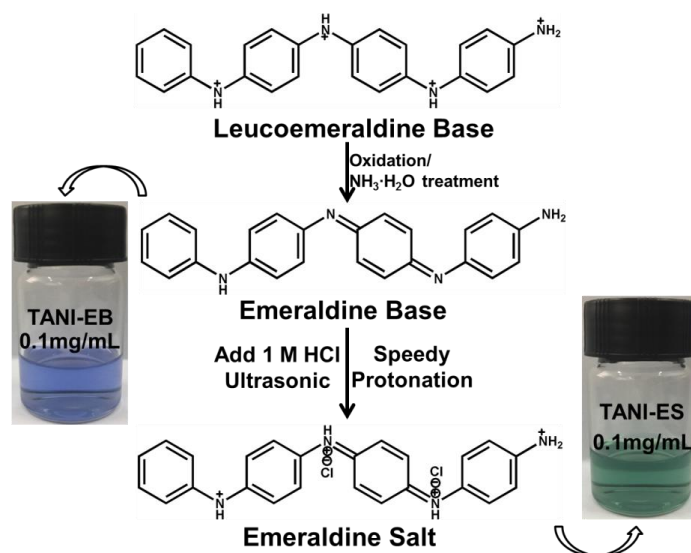

Figure 1. Preparation schematic representation and protonation interactions of the TANI nanofibers (samples of bottles were dispersed in the ethanol solution)

2.4 Preparation of TANI-ES nanofiber/epoxy anticorrosion composite coatings

In this work, the content of TANI-ES nanofiber was predesigned as 0.5 wt% and 1.0 wt% in epoxy coatings and pure epoxy coating as blank. All the ingredients except curing agent were mixed based on the requisite proportion and dispersed by using a high-speed agitator (1000 r/min) for 2 h at room temperature. Oily polyamide curing agent and epoxy resin (E44) with a ratio of 1:4 was mixed. Then the mixture was adjusted to the fitted viscosity. The blank (pure epoxy) was also prepared as the same method. The Q235 steel electrodes (experimental region of steel sample: 10 mm × 10 mm) were treated by ultrasonic cleaning machine in absolute ethanol repeatedly and polished with 400-grit, 800-grit and 1200-grit sand papers. Every mixed composite was coated on the steel electrodes via a bar coater (20μm) for EIS measurements (The coating thickness: 20 ± 2μm). The coatings with pure epoxy, 0.5 wt % and 1.0 wt % were marked as blank, nanofiber-0.5# and nanofiber-1#. The prepared coatings were cured for 72 h under room temperature until the coatings were fully cured.

2.5 Characterization of the prepared TANI-EB and TANI-ES nanofiber

The scanning electron microscope (SEM) images of TANI nanofibers and coatings' fracture surfaces were performed by HITACHI S4800. And the morphologies of TANI nanofibers were also exhibited by the scanning probe microscope (SPM, Dimension 3100). The UV–vis spectrum was obtained on Lambda 950 spectroscope. The conductivity of TANI nanofibers was measured by four-point probe technique (CRESBOX).

2.6 Electrochemical tests of anticorrosion composite coatings

Electrochemical measurements were conducted in three electrodes system on CHI-660E electrochemical workstation and the tests (open circuit potential (OCP) and electrochemical impedance spectroscopy (EIS)) were all proceeded in 3.5 wt % NaCl solution. The EIS parameters were collected during the frequency region of 10^{-2} - 10^5 Hz and alternating current (AC) signal with a sine wave of 20 mV amplitude. In this work, scanning vibrating electrode technique (SVET) test instrument was from AMETEK. The microelectrode parameters have the amplitude of 30μm vibrated and frequency of 80 Hz in perpendicular direction to the surface (scan area: 2000 μm × 2000 μm and 21 × 21 points X and Y-axis). Artificial defects exposed the carbon steel substrate surface were cutted on the blank, nanofiber-0.5# and nanofiber-1# coatings by a knife. The artificial defects' distance was around 2 mm.

2.7 Salt Spray Tests of anticorrosion composite coatings

The Q235 steel sheets were polished by the sand papers of 400, 600 and 800 grids, and the size of sheets were 4 cm × 2.5 cm × 0.1 cm. The scratch length of prepared samples was 2.5 cm and thickness of coatings was at around 70 μm. Salt spray studies were tested with CCT1100 by using salt spray of 3.5 wt % NaCl solution, which was made by Q-Lab Corporation.

3. RESULTS AND DISCUSSION
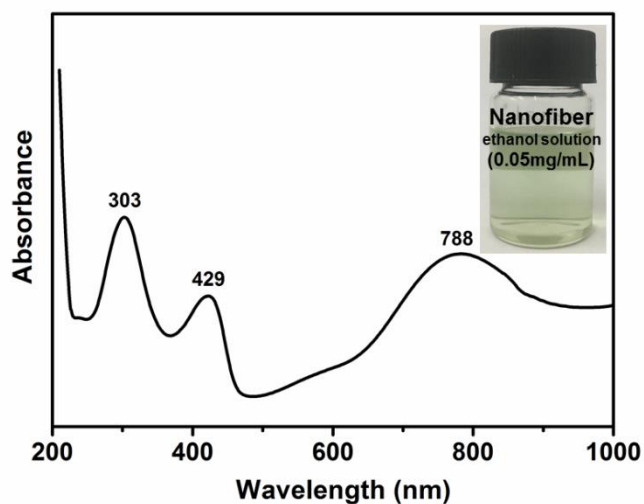
3.1 Characterization of TANI-ES nanofiber

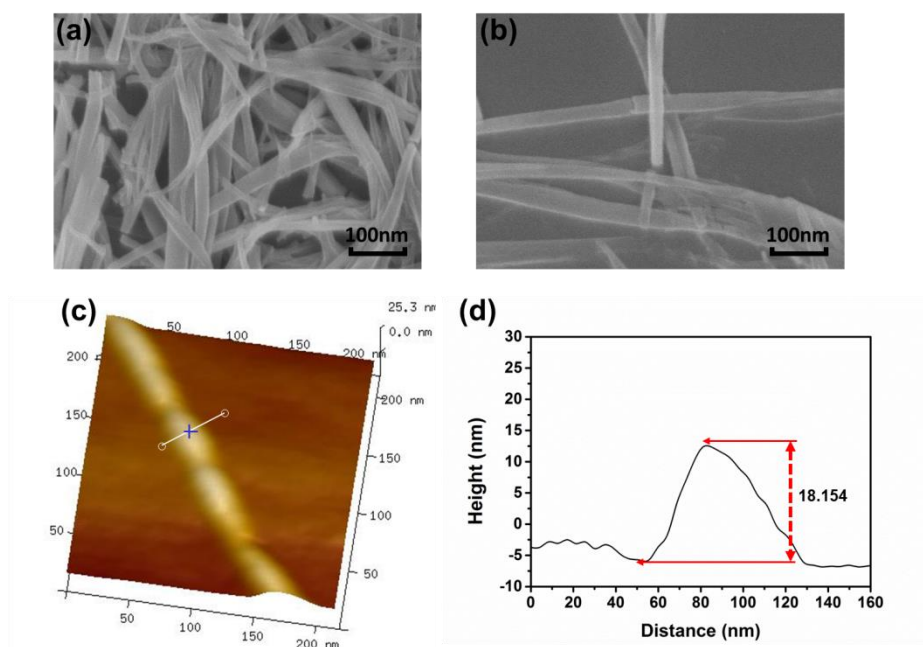**Figure 2.** UV–vis spectra of TANI-ES nanofibers

Figure 3. Typical (a, b) SEM and (c, d) SPM images of TANI-ES nanofibers

The absorption spectrum of the TANI-ES nanofiber was recorded on a UV-vis spectrometer. The UV-vis pattern of nanofiber in the range from 200 to 1000 nm was showed in Fig. 2 (the concentration of testing solution: 0.05 mg/mL, solvent: absolute ethanol). It displayed three characteristic peaks at about 303, 429 and 788 nm that were corresponded to the typical π-π*, polaron-π* and π-polaron transitions, respectively. It implied that the nanofibers are doped to form conductive

emeraldine salt state [30, 31]. The conductivity of TANI nanofiber was measured to 90.78 mS/cm by using four-point probe technique. The TANI-ES nanofiber exhibited good solubility in ethanol, making it possible to homogenously imbedded into epoxy matrix.

The typical TEM and SPM images of TANI-ES nanofiber were shown in Fig. 3. In Fig. 3a and b, the as-prepared sample possessed a nanofibrous structure with even width of ca. 50 nm and length up to several hundreds of nanometers. For SPM morphologies, it displayed the thickness up to approximately 18.2 nm, confirming that we had succeeded in making self-assembly tetraaniline HCl-doped nanofibers.

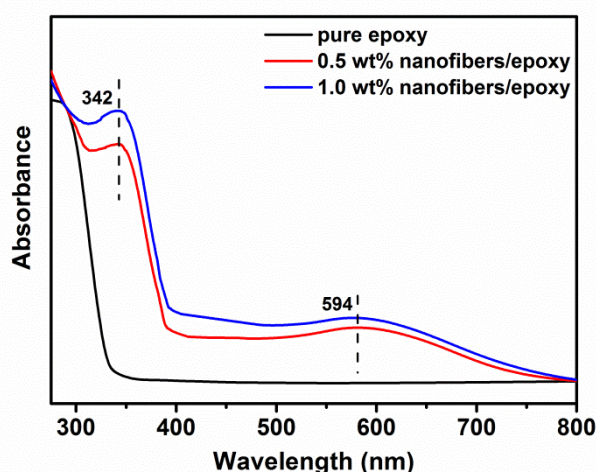*3.2 Characterization of TANI-ES nanofiber/epoxy anticorrosion coating*

Figure 4. UV-vis spectra of blank, nanofiber-0.5# and nanofiber-1# coatings

For further investigation to the TANI-ES nanofiber in mixture coating, UV-vis patterns of pure epoxy, nanofiber-0.5# and nanofiber-1# coatings were tested by even and transparent coatings, which were coated on thin sheet glass (material quality: quartz). For blank sample in Fig. 4, there was no apparent absorption peaks found in the wavelength from 300 nm to 800 nm. Nevertheless, the obvious peaks were found in nanofiber-0.5# and nanofiber-1# coatings UV-vis spectra, which were associated the absorption of TANI-ES. In detail, the strong peak at 342 nm referred to the typical π-π*, and the weak peak at about 594 nm was corresponded to polaron band transition of TANI-ES nanofiber [18, 32].

To further investigate the dispersion ability of nanofibers in the epoxy coating, the SEM images of different coatings' cross-sections were exhibited in Fig. 5. For pure epoxy coating in Fig. 5a, there existed some obvious defects on the fractured surface, for example, tube-like breaking traces and ineluctable tiny air bubbles formed during the curing process were observed. These slight faults and air bubbles were the key issue of anti-corrosion function of coating. Nevertheless, micaropores can hardly be seen on the fracture surface of nanofiber-0.5#, implying that TANI nanofiber can efficiently fill the

microcavities in the matrix (Fig. 5b). As a comparison, we can see much more wrinkles on the fracture surface of nanofiber-1# (Fig. 5c), it is probably because the large amount of nanofibers induced more crack propagation. Therefore, the above studies have shown that 0.5 wt% nanofiber has preferable dispersion state in epoxy coating matrix.
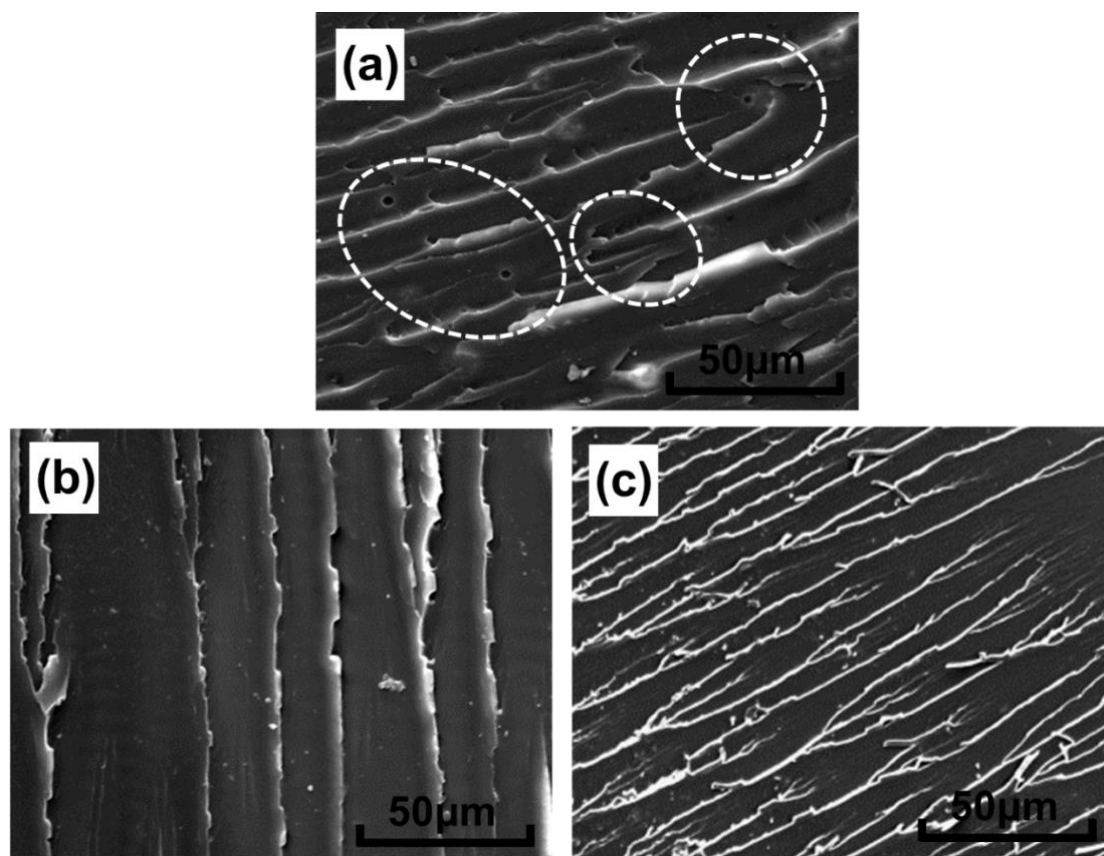

Figure 5. SEM images of different coatings' fracture surfaces: (a) blank, (b) nanofiber-0.5# and (c) nanofiber-1#

3.3 Open circuit potential measurements

The variation of open circuit potential (OCP) as function of immersion time for as-prepared coatings in 3.5 wt% NaCl solution was exhibited in Fig. 6. As a whole, decline trend of three broken lines implied that the NaCl solution has permeated gradually into organic coatings. In terms of pure epoxy coating, OCP values decreases steadily from -0.001 V vs. SCE to -0.497 V vs. SCE after immersion in 3.5 wt% NaCl solution of 40 days. However, during the next 60 days, the obvious increase in OCP value (from-0.497 V vs. SCE to -0.429 V vs. SCE) was owing to the accumulation of corrosion products on the steel substrate surface.
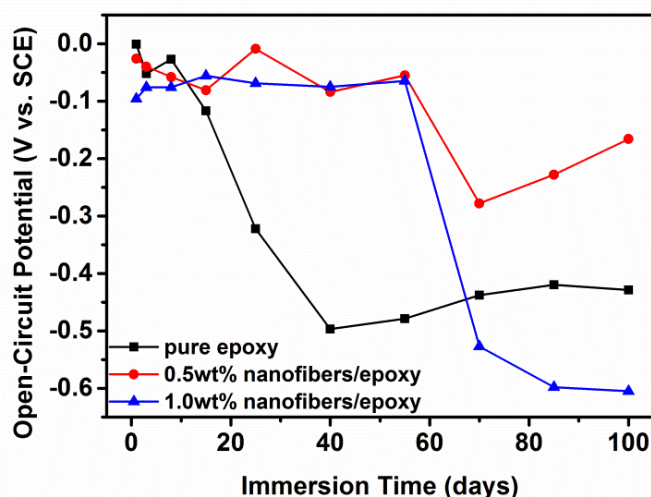
Figure 6. Open circuit potential (OCP) of different coatings in 3.5 wt % NaCl solution for 100 days

For nanofiber-1#, there was a sharp change of OCP from 55 days (-0.065 V vs. SCE) to 70 days (-0.527 V vs. SCE), indicating that water penetration was serious. It could be concluded that the excess nanofibers in the coating might deteriorate the coating integrity. In addition, it is worthwhile to note that the final OCP value of nanofiber-0.5# (-0.166 V vs. SCE) showed higher value of OCP than those of the blank (-0.429 V vs. SCE) and nanofiber-1# (-0.605 V vs. SCE), indicated the best anti-corrosion potentiality.

3.4 Electrochemical impedance spectroscopic analysis

The electrochemical impedance characterization of TANI-ES nanofiber/epoxy was studied by electrochemical impedance spectroscopy (EIS) during the immersion in 3.5 wt% NaCl solution (Fig. 7). In point of Nyquist plot of blank coating, the shrinking capacitive arcs were displayed in Fig. 7a. In addition, the radii of capacitive arcs dropped greatly from 15 days to 25 days immersion in 3.5 wt% NaCl solution, implying that the corrosion resistance of coated steel evidently decreased due to pure epoxy coated defects, e.g. tiny air bubble. But unlike pure epoxy coating, as we can see in the Fig. 7c and 7e, the high capacitive loop radii of nanofiber-0.5# and nanofiber-1# was all kept for around 55 days, which proved that epoxy coatings containing nanofibers possessed excellent anti-corrosion behavior.

For further study of anti-corrosion behavior of samples, the Bode plots were also shown in Fig. 7. As a rule, for typical electrochemistry analysis, the other index of coating anticorrosion behavior was the impedance values at the lowest frequency (frequency parameter: 0.01 Hz) [19, 33] and the higher measured impedance value indicated the better anticorrosion capability of coatings. In terms of early impedance, $|Z|_{f=0.01Hz}$ value of blank sample, nanofiber-0.5# and nanofiber-1# were up to 3.07×10^{10}, 1.03×10^{11} and 4.51×10^{9} Ω cm^2, respectively. Furthermore, for Bode plot of blank sample in Fig. 7b, the impedance sharply declined from 15 days (1.77×10^{11} Ω cm^2) to 25 days (3.60×10^{7} Ω cm^2) with NaCl solution immersion, which showed relatively inferior corrosive resistance. However,

nanofiber-0.5# (3.97×10^8 Ω cm^2) and nanofiber-1# (1.25×10^8 Ω cm^2) are both displayed the higher mid-term impedance value. In the later period of corrosion process during 100 days' immersion, the $|Z|_{f=0.01Hz}$ values for pure epoxy, nanofiber-0.5# and nanofiber-1# were 9.22×10^6, 3.11×10^8 and 3.21×10^7 Ω cm^2, respectively. On the whole, composite coating with 0.5 wt% TANI-ES nanofibers possessed the highest initial and final impedance values, which indicated the best corrosion-proofing ability after 100-days immersion.
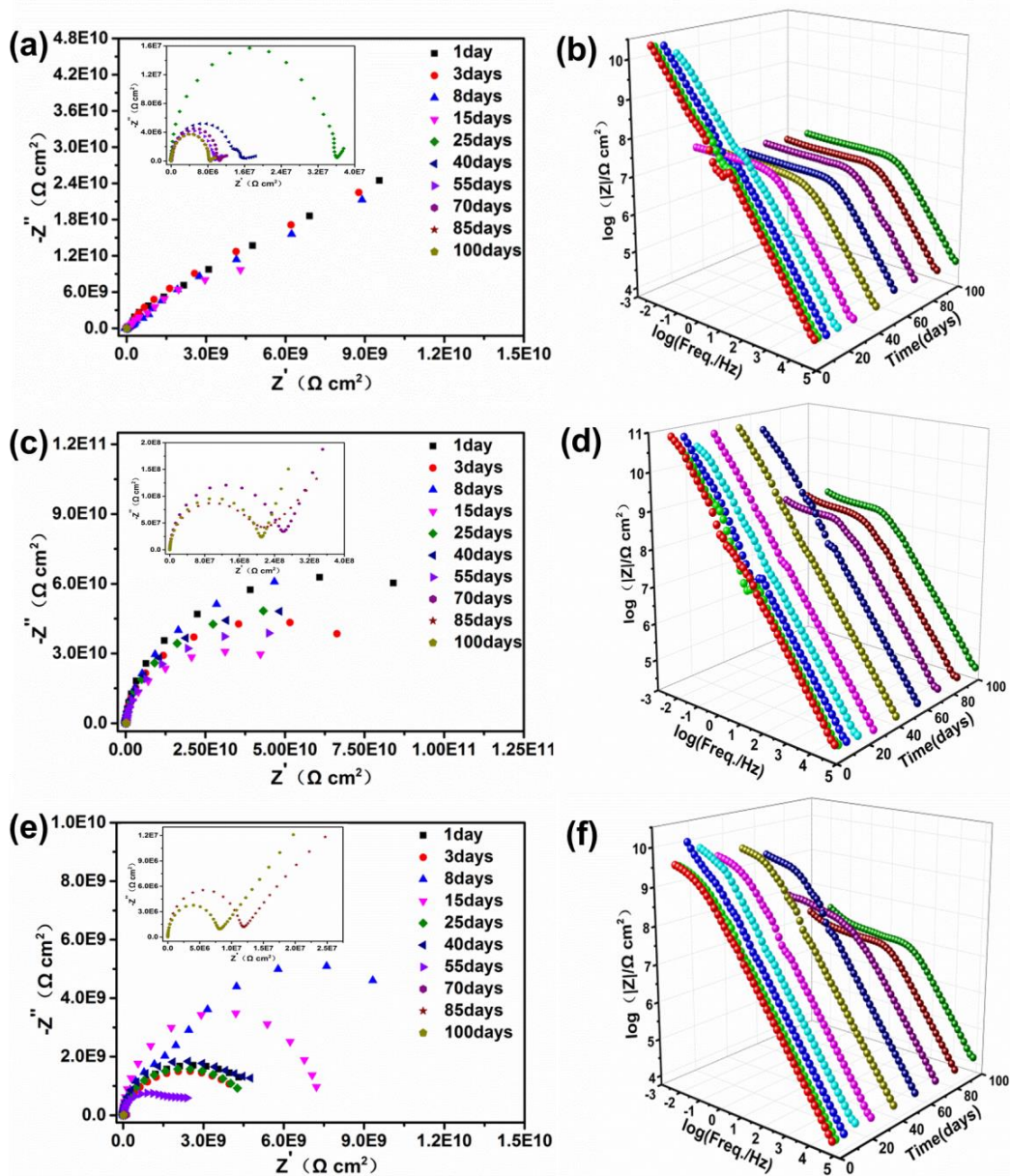

Figure 7. Nyquist and Bode plots of the samples coated with different coatings (a, b) blank, (c, d) nanofiber-0.5#, (e, f) nanofiber-1#

Fig. 8 exhibited fitted Electrical equivalent circuit models of EIS data, which were simulated by ZSimpWin 3.30 analysis Software. In equivalent circuit, R_s, R_c and R_{ct} were solution resistance, coating resistance and charge-transfer resistance. For capacitance section, corresponding Q_c and Q_{dl}

represented coating capacitance and double layer capacitance. The initial immersion EIS plots were suited for circuit-a (Fig. 8a) due to the NaCl solution were unable to arrive the coatings' interior. After incipient immersion, corrosion medium permeated into the solution/coating or coating/metal base [34, 35]. This circumstance was fit for circuit-b (Fig. 8b).
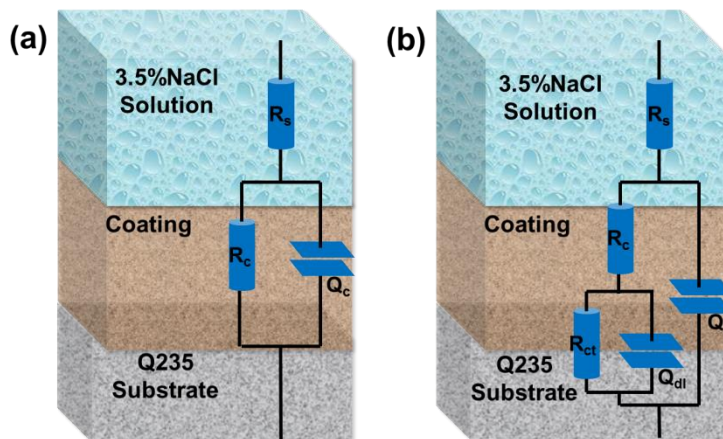

Figure 8. Electrical equivalent circuit models (a, b) with immersion in 3.5 wt% NaCl solution for 100 days
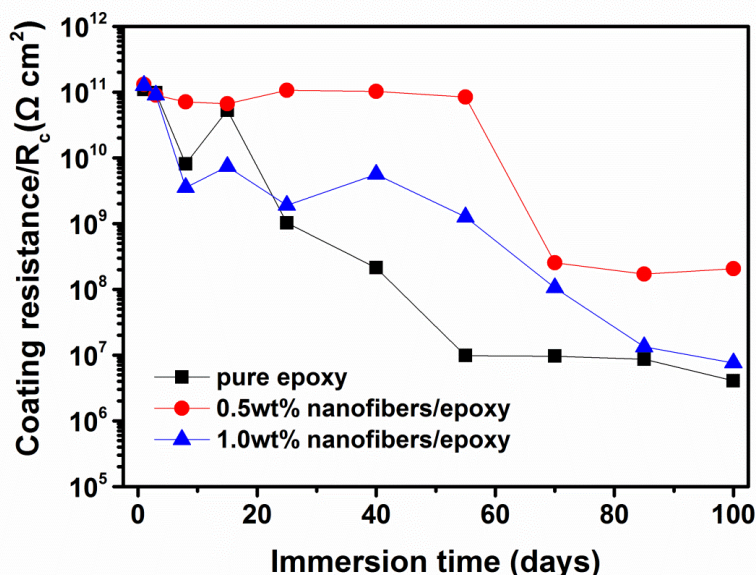

Figure 9. Fitted results of coating resistance for different coatings in 3.5 wt% NaCl solution for 100 days

Fitted results of coating resistance (R_c) for different coatings in 3.5 wt% NaCl solution after 100 days immersion were presented in Fig. 9. In general, R_c declined in the wake of increasing soaked time due to the NaCl solution's permeation and degradation of epoxy coating [36-38]. For pure epoxy coating, the coating resistance decreased from 1.09×10^{11} to $4.05 \times 10^6 \, \Omega \, cm^2$. In terms of composite organic coating, nanofiber-0.5# and nanofiber-1# had the coating resistance values of 2.01×10^8 and $7.61 \times 10^6 \, \Omega \, cm^2$ of immersed final stage. Obviously, nanofiber-0.5# coating sample was two orders of

magnitude higher than those of blank sample and nanofiber-1#, implying that blank and nanofibers-1# had weak anticorrosion performance after the immersion of 100 days.
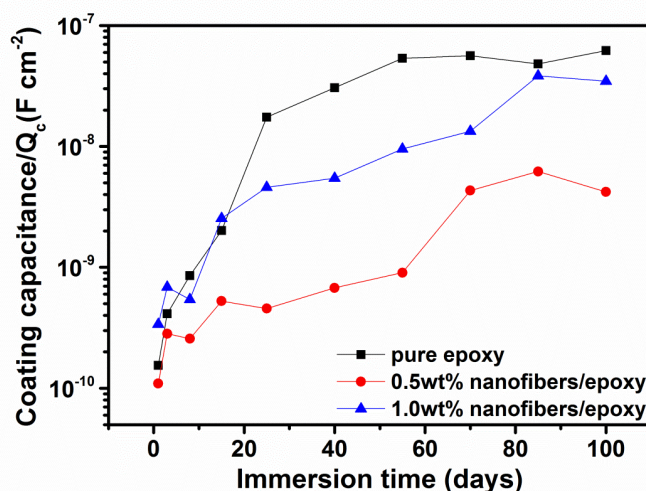

Figure 10. Fitted results of coating capacitance for different coatings in 3.5 wt% NaCl solution for 100 days

Generally, coating capacitance (Q_c) represented the absorption of water solution, and the coating was apt to breach with the permeation of water, which led to the loss of the shielded function [18]. As we can see in Fig. 10, the values of Q_c for different coatings in 3.5 wt% NaCl solution after 100 days immersion all presented upward tendency on the whole. In detail, the Q_c measured values for blank and nanofiber-1# have enhanced to 6.21×10^{-8} and 3.47×10^{-8} F cm^{-2} after immersion of 100 days, respectively, owing to the coating was heavily penetrated by NaCl electrolyte. However, it was obvious that terminal Q_c value (4.21×10^{-9} F cm^{-2}) of nanofiber-0.5# were much lower than those of the above two coatings', which indicated that the less 3.5 wt% NaCl solution permeated into composite coating. The aggressive medium permeated into coatings deal to the raise of Q_c, because water possessed the higher local dielectric constant value than coating [39, 40]. Thus, in analysis of Q_c, nanofiber-0.5# possessed the lowest Q_c value during the entire immersion time, implying the satisfactory corrosion barrier property.

3.5 Scanning vibrating electrode technique analysis

For further study the corrosion resistance effect of the coatings with TANI-ES nanofibers, the scanning vibrating electrode technique (SVET) was used for characterizing voluntary corrosion protection and the local area corrosion behaviors by observation of current density distribution [41-43].

Experiment measured potential difference converted to the local-area corrosion current density (i_{corr}), and conversion formula was shown as follow:

$$i_{corr} = -\Delta\varphi\,\frac{k}{d}\,(\mu A\ cm^{-2}) \qquad\qquad (1)$$

where the Δφ is the electric potential drop, k is the electrolyte conductivity and d is the vibration amplitude.
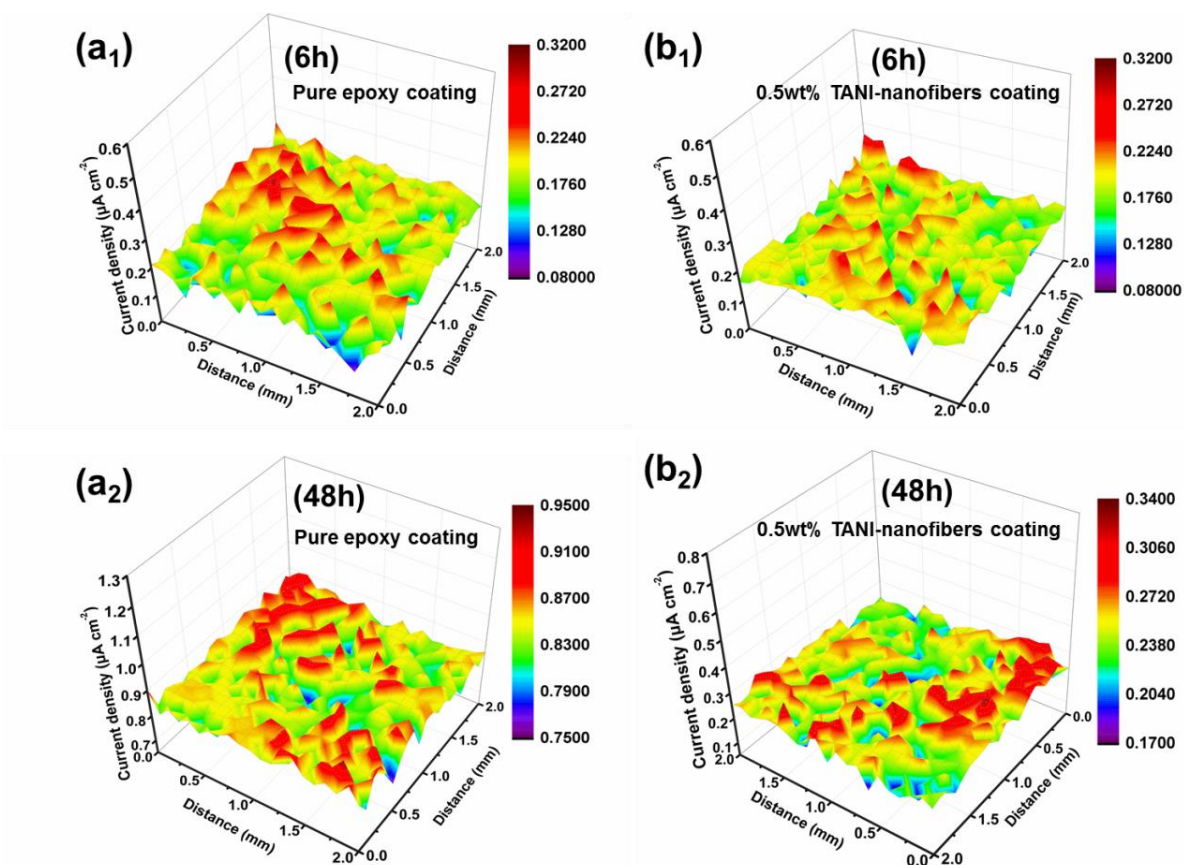

Figure 11. SVET 3D current density distribution maps of coated steels immersed in 3.5wt % NaCl solution for 1 hour and 24 hours. (a$_1$, a$_2$) Blank and (b$_1$, b$_2$) nanofiber-0.5#, unit of current density: μA cm^{-2}.

To be brief, the electrochemical reactions of artificially scratches with immersion in aggressive medium led to the obvious increase in anodic local-area current density. The current density colorful maps after 6 h and 48 h with immersion in 3.5 wt% NaCl solution aggressive medium solution for pure epoxy and nanofiber-0.5# were displayed in Fig. 11. As we can see in the Fig. 11a$_1$ and 11b$_1$, the similar distribution of colorful maps and obvious corrosion trail (red part of ridge-shape) were shown, which indicated that pure epoxy and nanofiber-0.5# had the same initial anodic current density conditions after 6 hours of immersion in the corrosion medium. With the extension of immersion time, the corrosion current density increased generally. As shown in Fig. 11a$_2$, the corrosion current density notably increased after 48 hours exposure to 3.5 wt% NaCl solution. By comparison, there was no palpable anodic corrosion current change (Fig. 11b$_2$) for the nanofiber-0.5# coating, indicating that corrosion behavior was restrained successfully with the existence of TANI-ES nanofiber. In addition, SVET measurement corroborated that conducting polymer fillers played a key role in anodic current density at artificially scratches test region.

3.6 Salt Spray Test

To further analyze the anticorrosion performance of TANI-ES containing epoxy coating, the images of epoxy coating without and with 0.5 wt% and 1 wt% TANI-ES after salt spray test for 48, 120 and 360 hours were presented in Figure 12. General, salt spray test was used for evaluating corrosion resistance of conducting polymer composite coatings [44-46]. For neat epoxy coating, it could also be easily observed that the coating suffered rapid and severe corrosion, including coating bubbling, inside corrosion with black rust and massive reddish yellow rust layers on the artificial scratch. However, the 0.5 wt% nanofiber coating effectively restrained sample bubbling and formation of corrosion production. In addition, nanofiber-1# also produced bubble and some rust because excess of nanofibers led to slightly defects and micropores inside the coating. By comparison, the 0.5 wt% nanofiber containing coating had a slight rust formation and possessed excellent salt-fog-resistance capability, proved that a small quantity of conducting polymer filler added into epoxy coating can give better salt fog resistance performance.
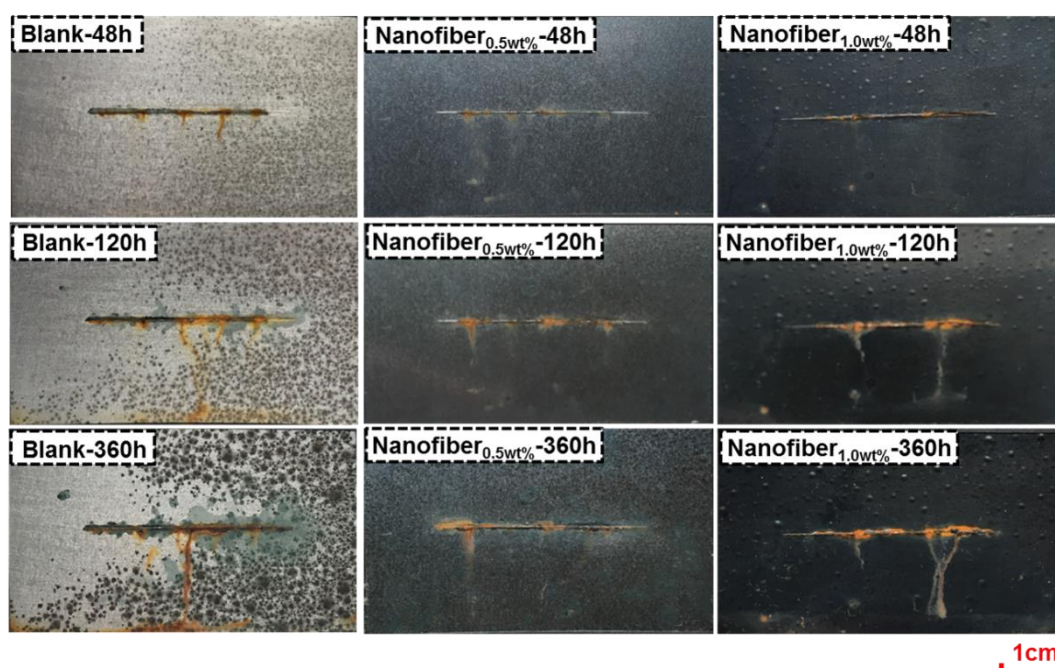

Figure 12. Photographs of pure epoxy, nanofiber-0.5# and nanofiber-1.0# coating samples after 48, 120 and 360 h exposure to salt spray test

4. CONCLUSIONS

In our work, processable emeraldine salt of tetraaniline nanofiber (TANI-ES) was prepared via suppermolecular assembly chemistry, making it suitable as processable additive for primer coatings. Epoxy coating pigmented with 0.5 wt% and 1.0 wt% TANI-ES were successfully prepared by curing reaction of epoxy E44, polyamide hardner with the existence of TANI-ES. The corrosion behavior of the coatings without and with 0.5 wt% and 1.0 wt% TANI-ES on Q235 in the 3.5 wt% NaCl solution

was investigated by open circuit potential (OCP) test, electrochemical impedance spectroscopy (EIS) measurements, scanning vibrating electrode technique (SVET) and salt spray test. The comprehensive results implied that epoxy coating blended with 0.5 wt% TANI-ES nanofiber showed impressive anticorrosion performance and salt fog resistance. The present study offers a novel method to prepare the processable conducing polymer and further potential applications as conductive pigment for enhancing the anticorrosive properties of epoxy based primer coatings.

References

1. A. M. Atta, M. I. Abdou, A. A. A. Elsayed, M. E. Ragab, *Prog. Org. Coat.*, 63 (2008) 372-376.
2. A. Omrani, *Chem. Eng. Commun.*, 202 (2015) 1389-1396.
3. L. Tang, J. Whalen, G. Schutte, C. Weder, *ACS Appl. Mater. Interfaces*, 1 (2009) 688.
4. C. Chen, S. Qiu, M. Cui, S. Qin, G. Yan, H. Zhao, L. Wang, Q. Xue, *Carbon*, 114 (2017) 356-366.
5. F. Deflorian, I. Felhosi, *Corros.*, 59 (2003) 112-120.
6. M. Martí, G. Fabregat, D.S. Azambuja, C. Alemán, E. Armelin, *Prog. Org. Coat,.* 73 (2012) 321-329.
7. J. H. Park, G. D. Lee, A. Nishikata, T. Tsuru, *Corros. Sci.*, 44 (2002) 1087-1095.
8. D. Das, *Paintindia*, 64 (2013) 73.
9. M. I. Khan, A.U. Chaudhry, S. Hashim, M.K. Zahoor, *Chem. Eng. Res. Bull.*, 14 (2010) 73-86.
10. T. Pan, *Spectrosc. Lett.*, 46 (2013) 268-276.
11. F. Beck, E. Abdelmula, M. Dahlhaus, *Electrochim. Acta*, 45 (2000) 3423-3429.
12. Z. Huang, A. Pencheng Wang, A.G. Macdiarmid, Y.X. And, G. Whitesides, *Langmuir*, 13 (2005) 6480-6484.
13. C. Peng, G.Z. Chen, J. Jin, *Electrochim. Acta*, 53 (2008) 525-537.
14. A. Olad, R. Nosrati, *Prog. Org. Coat.*, 76 (2013) 113-118.
15. J. Fang, K. Xu, L. Zhu, Z. Zhou, H. Tang, *Corros. Sci.*, 49 (2007) 4232-4242.
16. M. Kraljić, Z. Mandić, L. *Duić, Corros. Sci.*, 45 (2003) 181-198.
17. S. Qiu, C. Chen, W. Zheng, W. Li, H. Zhao, L. Wang, *Synth. Met.*, 229 (2017) 39-46.
18. S. Qiu, C. Chen, M. Cui, W. Li, H. Zhao, L. Wang, *Appl. Surf. Sci.*, 407 (2017) 213-222.
19. C. Chen, *Int. J. Electrochem. Sci.*, 12 (2017) 3417-3431.
20. F. Yang, *Int. J. Electrochem. Sci.*, 10 (2017) 7469-7480.
21. B. Chen, J. Ma, L. Gu, S. Liu, H. Zhao, H. Yu, J. Chen, *Int. J. Electrochem.*, 10 (2015) 9154-9166.
22. F. Yang, *Int. J. Electrochem. Sci.*, 12 (2017) 5349-5362.
23. L. Zang, Y. Che, J.S. Moore, Accounts of Chemical Research 40 (2009) 1596-1608.
24. H. Kim, T. G. Kim, J. W. Park, *Macromol. Res.*, 21 (2013) 815-820.
25. B. O. Alexander, G. Wu, J. S. Haataja, B. Felicitas, F. Natalie, A. M. Seddon, R. L. Harniman, R. M. Richardson, I. Olli, Z. Xi, J. Am. Chem. Soc., 137 (2015) 14288-14294.
26. Y. Li, W. He, J. Feng, X. L. Jing, *Colloid Polym. Sci.*, 290 (2012) 817-828.
27. W. Lv, J. T. Feng, W. Yan, C. F. J. Faul, *J. Mater. Chem. B*, 2 (2014) 4720-4725.
28. S. P. Surwade, S. R. Agnihotra, V. Dua, N. Manohar, S. Jain, S. Ammu, S. K. Manohar, *J. Am. Chem. Soc.*, 131 (2009) 12528.
29. L. Gu, S. A. Liu, H. C. Zhao, H. B. Yu, *Rsc. Adv.*, 5 (2015) 56011-56019.

30. W. Lyu, J. Feng, W. Yan, C.F.J. Faul, *J. Mater. Chem. C*, 3 (2015) 11945-11952.
31. W. Lv, J. Feng, W. Yan, C. F. J. Faul, *J. Mater. Chem. B*, 2 (2014) 4720-4725.
32. A. Airoudj, D. Debarnot, B. Beche, F. Poncin-Epaillard, *Talanta*, 77 (2009) 1590-1596.
33. S. Qiu, W. Li, W. Zheng, H. Zhao, L. Wang, *ACS Appl. Mater. Interf.*, 9 (2017) 34294-34304.
34. Y. Zhang, Y. Shao, T. Zhang, G. Meng, F. Wang, *Prog. Org. Coat.*, 76 (2013) 804-811.
35. X. Yan, Z. Tai, J. Chen, Q. Xue, *Nanoscale*, 3 (2011) 212.
36. X. Liu, J. Xiong, Y. Lv, Y. Zuo, *Prog. Org. Coat.*, 64 (2009) 497-503.
37. Y. Hao, F. Liu, E. H. Han, *Prog. Org. Coat.*, 76 (2013) 571-580.
38. F. Mansfeld, *Electrochim. Acta*, 35 (1990) 1533-1544.
39. P. Kern, A. L. Baner, J. Lange, *J. Coat. Technol.*, 71 (1899) 67-74.
40. A. Kosari, M. H. Mnoayed, A. Davoodi, *Corros. Sci.*, 78 (2014) 138-150.
41. Y. H. Liu, J. B. Xu, J. T. Zhang, J. M. Hu, *Corro. Sci.*, 120 (2017) 61-74.
42. M. Mouanga, F. Andreatta, M.E. Druart, E. Marin, L. Fedrizzi, M.G. Olivier, *Corros. Sci.*, 90 (2015) 491-502.
43. R. B. Vichessi, F. Calegari, C. E. B. Marino, M. A. C. Berton, SVET characterization of corrosion process in carbon steel 1020, *Int. Seminar Ind. Innovation Electrochem.*, (2016) 11-20.
44. Z. B. Bao, Q. M. Wang, W. Z. Li, J. Gong, T. Y. Xiong, C. Sun, *Corros. Sci.*, 50 (2008) 847-855.
45. F. Chen, P. Liu, *ACS Appl. Mater. Interf.*, 3 (2011) 2694-2702.
46. B. Ramezanzadeh, M.H. Mohamadzadeh Moghadam, N. Shohani, M. Mahdavian, *Chem. Eng. J.*, 320 (2017) 363-375.